Projected Changes of Precipitation Characteristics Depend on Downscaling Method and Training Data: MACA versus LOCA Using the U.S. Northeast as an Example

GUILING WANG,[a,b] CHRISTINE J. KIRCHHOFF,[a] ANJI SETH,[c] JOHN T. ABATZOGLOU,[d] BEN LIVNEH,[e,f] DAVID W. PIERCE,[g] LORI FOMENKO,[a] AND TENGYU DING[a]

[a] *Department of Civil and Environmental Engineering, University of Connecticut, Storrs, Connecticut*
[b] *Center for Environmental Science and Engineering, University of Connecticut, Storrs, Connecticut*
[c] *Department of Geography, University of Connecticut, Storrs, Connecticut*
[d] *Department of Geography, University of Idaho, Moscow, Idaho*
[e] *Department of Civil, Environmental, and Architectural Engineering, University of Colorado Boulder, Boulder, Colorado*
[f] *Cooperative Institute for Research in Environmental Sciences, University of Colorado Boulder, Boulder, Colorado*
[g] *Scripps Institution of Oceanography, La Jolla, California*

(Manuscript received 18 November 2019, in final form 29 May 2020)

ABSTRACT: This study compares projected changes of precipitation characteristics in the U.S. Northeast in two analog-based climate downscaling products, Multivariate Adaptive Constructed Analogs (MACA) and Localized Constructed Analogs (LOCA). The level of similarity or differences between the two products varies with the type of precipitation metrics. For the total precipitation amount, the two products project significant annual increases that are similar in magnitude, spatial pattern, and seasonal distribution, with the largest increases in winter and spring. For the overall precipitation intensity or temporal aggregation of heavy precipitation (e.g., number of days with more than one inch of precipitation, the simple intensity index, and the fraction of annual precipitation accounted for by heavy events), both products project significant increases across the region with strong model consensus; the magnitude of absolute increases are similar between the two products, but the relative increases are larger in LOCA due to an underestimation of heavy precipitation in LOCA's training data. For precipitation extremes such as the annual maximum 1-day precipitation, both products project significant increases in the long-term mean, but the magnitude of both the absolute and relative changes are much smaller in LOCA than in MACA, indicating that the extreme precipitation differences in the training data are amplified in future projections as a result of the analog-based downscaling algorithms. The two products differ the most in the intensity and frequency of rare extremes (e.g., 1-in-20-years events) for which MACA projects significant increases while the LOCA-projected changes are inconclusive over much of the study area.

KEYWORDS: Climate prediction; Hydrologic cycle; Hydrometeorology; Bias; Interpolation schemes; Statistical techniques

1. Introduction

State and local governments and decision-makers across a range of sectors including agriculture, transportation, energy, and water are increasingly seeking place-based climate change information to inform climate adaptation planning (Bierbaum et al. 2013; Mach and Field 2017; Kirchhoff et al. 2019). Yet, climate change projections derived from global climate models (GCMs) with a typical spatial resolution of ~100–300 km, or from dynamical downscaling using regional climate models (RCMs) with a typical spatial resolution of 12–50 km (e.g., Giorgi et al. 2009; Giorgi 2019; Mearns et al. 2012; Ruti et al. 2016; Zobel et al. 2018), are often too coarse to inform local adaptation decisions (e.g., Wilby and Dessai 2010). Finer-resolution dynamical downscaling output is often limited to small domain, short length of model integration, or small ensemble size (e.g., d'Orgeville et al. 2014; Prein et al. 2017). The computational efficiency of statistical downscaling, which is based on empirical relationships between local variables and large-scale features, enables the creation of downscaled data for a large ensemble of GCMs and RCMs and correction of systematic biases in surface meteorological variables in these models (Maraun et al. 2010). Given these advantages, statistical downscaling is frequently used to downscale GCMs and RCMs projections (of precipitation and temperature in particular) to local scales that might be more directly usable by state and local decision-makers (e.g., Maraun et al. 2010; Ning et al. 2012; Abatzoglou and Brown 2012; Ahmed et al. 2013).

Statistical downscaling assumes that the present-day observed relationship between local variables (predictant, e.g., precipitation, temperature) and large-scale features (predictors, e.g., pressure field, circulation pattern, humidity, or coarse-resolution version of the predictant) will hold in future climate. Many different statistical downscaling approaches have been developed, based on simple change factors, linear or nonlinear regression, self-organizing maps, quantile mapping, or analogs (e.g., Wood et al. 2004; Hewitson and Crane 2006; Fowler et al. 2007; Maurer et al. 2010; Stoner et al. 2012; Ahmed et al. 2013; Alder and Hostetler 2019). Some statistical downscaling approaches were developed for climate fields at monthly resolution, and some at daily resolution. For climate variables at the daily resolution, some widely used downscaling approaches underestimate precipitation extremes and fail to resolve the finescale spatial anomalies (see reviews in Bureau of Reclamation 2013; Gutmann et al. 2014; Mizukami et al. 2016). The constructed analogs approaches, including, for

Corresponding author: Guiling Wang, guiling.wang@uconn.edu

DOI: 10.1175/JHM-D-19-0275.1

example, the Multivariate Adaptive Constructed Analogs (MACA; Abatzoglou and Brown 2012) and the Localized Constructed Analogs (LOCA; Pierce et al. 2014, 2015), were developed to address such challenges. To downscale a GCM future daily field (using daily precipitation as an example), for each day of the model data, constructed analog techniques such as LOCA and MACA first identify multiple historical analog days (i.e., days from observational or reanalysis data that have large-scale features similar to the model data), and assume that the relationship between the regionally-averaged precipitation (e.g., precipitation at the GCM resolution) and precipitation at a particular point on the finer grid is the same in the future as it was on the selected historical analog day(s). A finer-resolution future precipitation field is then computed as the weighted average of finer-resolution observed precipitation among the analog days (Pierce et al. 2015). LOCA is considered an improved methodology over MACA in the choices of analogs and in how bias corrections are applied (see details in section 2). MACA and LOCA have been applied to daily output from a large ensemble of Coupled Model Intercomparison Project phase 5 (CMIP5) GCMs to derive three fine-resolution future climate projection databases for the United States: LOCA database using the Livneh et al. (2015) data as observational reference, MACA-M using gridMET (Abatzoglou 2013), and MACA-L using the Livneh et al. (2015) data as observational references.

LOCA and MACA climate projection databases include primary variables for surface climate (precipitation and temperature, among others), and have seen widespread application in climate change assessments and adaptation planning. For example, the LOCA database was used in the Fourth U.S. National Climate Assessment (Easterling et al. 2017) and the Massachusetts state climate assessment (Northeast Climate Adaptation Science Center 2018; https://necsc.umass.edu/projects/massachusetts-climate-change-projections); MACA-M was used in the U.S. Forest Service Resource Planning Act assessment (Joyce et al. 2018) and the Connecticut state climate assessment (e.g., Seth et al. 2019). Climate change assessments are undertaken in collaboration with decision-makers and other stakeholders to better align assessment outputs with the needs of potential users of those outputs (Cash et al. 2003; Kirchhoff et al. 2019). Assessments are often used to help decision-makers understand changes in future flood, drought, and other risks that in turn rely on data for precipitation characteristics defined at short temporal scales (such as precipitation intensity, frequency, and extremes at daily or hourly resolution) that are challenging to downscale and quantify. While the choice of database used in climate change assessments and adaptation planning often depends on the purpose of the assessment or the question being asked (Kotamarthi et al. 2016), too often databases are chosen with very little consideration of the effect that choice has on assessment findings. Uncertainty analyses, if included at all, primarily concerned GCM dependence and the representative concentration pathways (RCPs).

Independently of assessment processes, scholars have evaluated statistically downscaled datasets and found a strong dependence of monthly and annual precipitation on the specific downscaling method and observational reference data used (e.g., Mizukami et al. 2016; Alder and Hostetler 2019). Moreover, observational reference itself is subject to uncertainties related to spatially and temporally distributing gauge-based precipitation data to create a uniform, gridded product (e.g., Livneh et al. 2015; Ahmadalipour and Moradkhani 2017; Henn et al. 2018). Alder and Hostetler (2019) evaluated six different downscaled datasets including among others the MACA-M, MACA-L, and LOCA databases and compared monthly temperature and precipitation in the western United States. They found substantial differences in mountainous regions between the monthly products using different downscaling methods as well as between products using the same methods but different observational reference data, and attributed such differences to elevation-related bias correction and the inclusion of high-elevation data (Alder and Hostetler 2019). Independent of elevation, relative to monthly precipitation, precipitation characteristics defined at short temporal scales (such as precipitation intensity, frequency, and extremes at daily or hourly resolution) are even more challenging to quantify and are often more sensitive to specific downscaling procedures (e.g., Bürger et al. 2012, 2013; Wootten 2018). While state and national climate assessments have used LOCA or MACA-M to quantify changes in these precipitation characteristics related to flood risks (Easterling et al. 2017; Seth et al. 2019), no direct comparison of extreme indicators between the two databases has yet been undertaken. As a result, it is not clear how differences in downscaling approach and observational reference data may have influenced the final products and how the choice of a particular product may have influenced the assessment results. To fill this gap, the current study compares precipitation characteristics and their future changes derived from the MACA-M (simply referred to as MACA hereafter) and LOCA databases, and elucidates what may have caused the differences between these two products using the U.S. Northeast as a case study.

Theoretical analysis of Earth's energy and water budgets and atmospheric thermodynamics suggests that as global temperature rises, global precipitation amount and extreme precipitation intensity will increase, while precipitation frequency will decrease with longer dry spells between precipitating events (e.g., Trenberth 1999). This general notion has been supported by results from global climate model experiments (e.g., Kharin et al. 2013, 2018; Wang et al. 2017a; Pierce et al. 2013; Polade et al. 2014; Badger et al. 2018) and increasingly confirmed by observational evidence (e.g., Fischer and Knutti 2016). Within the United States, the Northeast has experienced the fastest regional increase of extreme precipitation, and the projected future increase of extreme precipitation is also the highest of the nation (Walsh et al. 2014; Easterling et al. 2017). Numerous studies have investigated the past and future changes of precipitation characteristics in the Northeast, including spatially lumped analysis, individual station-based analysis, and spatially distributed analysis using gridded data (e.g., Keim and Rock 2002; Groisman et al. 2004, 2005; Griffiths and Bradley 2007; Brown et al. 2010; Hodgkins and Dudley 2011; Kunkel et al. 2013; Horton et al. 2014; Janssen et al. 2014; Walsh et al. 2014; Thibeault and Seth 2014; Ning et al. 2015; Easterling et al. 2017). Differences among

past studies primarily concerned the magnitude and sometimes seasonality of changes, which depended on the specific time periods over which the changes were defined as well as the source of observational data and models for future projections. However, qualitatively, all past studies documented a shift toward a more flood-prone condition, including an observed or projected overall increase of precipitation amount and increase of heavy precipitation frequency and intensity.

The U.S. Northeast is home to several major metropolises, making the region especially vulnerable to extreme events from a socioeconomic perspective. And while state- and city-level climate change assessments (e.g., Boston, New York City, Massachusetts, and Connecticut) (Kirchhoff et al. 2019) seek to provide climate change information relevant to local metropolitan issues such as flooding and water quality, those tasked with undertaking climate assessments may lack information or knowledge on whether existing datasets are suitable for use in local assessments and how analytical results may depend on which specific database is used. Through comparing two major databases (MACA and LOCA) for the downscaled U.S. climate using the Northeast as an example, this study attempts to elucidate similarities and differences and their implications, and identify research needs for further development or improvement of climate downscaling methods and datasets to better serve society. Note that both MACA and LOCA have been independently documented elsewhere. The focus of this study is not on their individual credential. Instead, we focus on their similarity and differences as they relate to uncertainties in climate assessment. Section 2 briefly describes the MACA and LOCA data and methods and the global models chosen, and section 3 describes the precipitation indices definition and analysis method. Results are presented in section 4, followed by discussion and conclusions in section 5.

2. Data description

This study compares precipitation characteristics and their future changes derived from two statistically downscaled climate databases, LOCA and MACAv2-METDATA. Data from both products are available at daily resolution, cover the period 1950–2005 for historical runs and 2006–2100 for future experiments, and include both RCP4.5 and RCP8.5 future scenarios. LOCA, with a spatial resolution of 1/16° (~6 km), was developed by applying the LOCA approach (Pierce et al. 2014, 2015) to 32 GCMs using the Livneh et al. (2015) data as the observational reference for bias correction. MACAv2-METDATA (referred to as ''MACA'' hereafter for convenience), with a spatial resolution of 1/24° (~4 km), was developed by applying the MACA approach (Abatzoglou and Brown 2012) to 20 CMIP5 GCMs using gridMET (formerly known as METDATA; Abatzoglou 2013) during 1979–2012 as the observational reference for bias correction. In addition, the MACA approach was applied to the same 20 GCMs using Livneh et al. (2015) during 1950–2011 as the observational reference for bias correction, and the resulting product is referred to as MACA-L. LOCA and MACA-L share the same training data, and MACA and MACA-L share the same downscaling and bias correction method. While the focus of this study is on comparing LOCA and MACA, data from MACA-L are analyzed to help understand the differences between LOCA and MACA.

Both LOCA and MACA are among the more sophisticated statistical downscaling methods, involving bias correction utilizing a training meteorological dataset (i.e., the observational reference) and spatial downscaling utilizing constructed analogs. The two methods differ in the number of analogs used to determine the climate variable (especially precipitation) at each grid cell and the stages at which bias corrections are applied. The MACA method (Abatzoglou and Brown 2012) includes *epoch removal and replacement* at the beginning and end of the procedure, *constructed analogs* for downscaling, and *quantile mapping approach* to bias correction (*before* and *after* constructed analog downscaling); the downscaling process involves weighted averaging across multiple chosen analogs. The LOCA approach (Pierce et al. 2014, 2015) features several improvements related to the choice of analog(s) and how bias correction is conducted. Instead of averaging across multiple analogs chosen based on large-scale pattern, LOCA employs multiscale matching by first identifying the top 30 best large-scale analogs and then choosing among them a single analog that is the best match for the local area around the grid cell being downscaled; moreover, LOCA refines the bias correction approach to preserve each GCM's original climate change projections and to better represent variability and extremes at multiple time scales.

In addition to method, differences in training data also contribute to the differences between the MACA and LOCA databases. The gridMET data (Abatzoglou 2013; training data for MACA) are available from 1979 to present day at a 1/24° resolution, and the Livneh et al. (2015) data (training data for LOCA) are available from 1950 to 2013 at a 1/16° resolution. Precipitation in both datasets are based primarily on publicly available data from rain gauges. The two datasets have a very similar monthly climatology based on the Parameter-Elevation Regressions on Independent Slopes Model (PRISM; Daly et al. 1994) product, but can exhibit large differences in day-to-day variations based on the choice of stations used, gridding assumptions, and treatment for temporal distribution.

We used independent daily precipitation data from ten stations at water supply reservoirs in southwest Connecticut spanning the area 41.28°–41.54°N, 72.62°–73.06°W, to compare with the two gridded datasets. These data were provided by the Southwest Connecticut Regional Water Authority (RWA) and were from rain gauge stations not used in deriving either gridded product. Figure 1 shows the comparison during several extreme events, averaged across the RWA water supply area. The daily precipitation in gridMET agrees quite well with observations at the RWA stations, but the Livneh et al. (2015) data tend to underestimate heavy precipitation and overestimate precipitation on days immediately before and/or after heavy precipitation events (Fig. 1). This qualitative observation based on individual events is confirmed by precipitation statistics over the RWA area based on the three datasets during their overlapping period 2001–13 (Table 1). For example, in the RWA area, the Livneh et al. data overestimate the number of rainy days by ~40%, underestimate the number of heavy precipitation days (with more than one inch of rain)

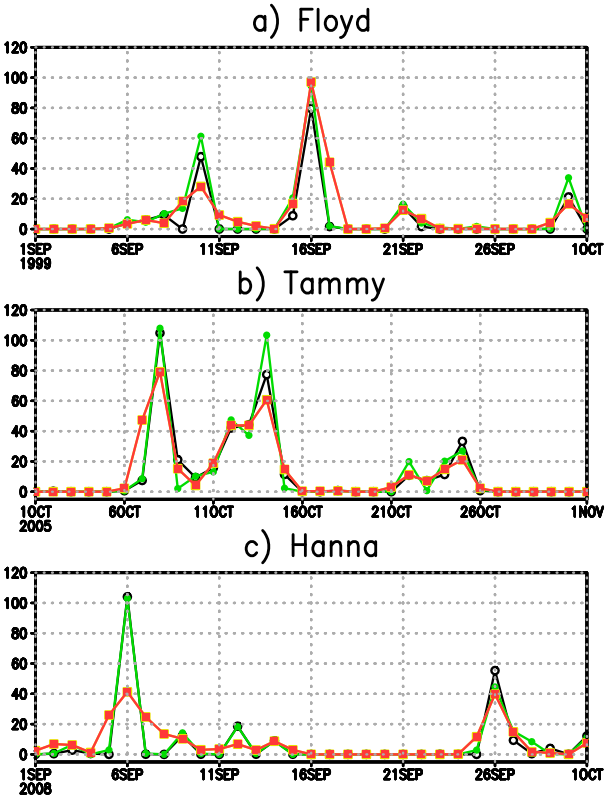

FIG. 1. (a)–(c) Spatial average of daily precipitation (mm) during the month of several extreme events: from gridMET (green), Livneh et al. dataset (orange), and rain gauges located at the Connecticut Regional Water Authority reservoirs (black).

by ~40%, and underestimate annual maximum 1-day precipitation by ~30% (Table 1). The inaccuracy of the Livneh et al. data is due to the use of a linear split of each recorded 24-h precipitation amount into two calendar days in data production (rather than using the simple nonoverlapping 24-h records for which the exact calendar day does not matter). When precipitation is aggregated over several days or a longer time period, the difference between the two datasets becomes negligible (Table 1). This comparison holds elsewhere too. For example, averaged over the common period of 34 years (1980–2013), the annual maximum 1-day precipitation (R1d) in the Livneh et al. (2015) data is much lower than in gridMET (Fig. 2). However, the maximum 5-day precipitation is almost identical between the two, and so is the annual total precipitation (Table 1 and Figs. 2 and 3).

Both MACA and LOCA include downscaled climate data from a large number of global climate or Earth system models. Global models are known to produce a large spread in their future projections, due to model dependence of both the climate sensitivity (defined based on the global average temperature response) and the spatial pattern of such response (e.g., Knutti et al. 2010; Tebaldi et al. 2011; Miao et al. 2014). A multimodel ensemble average is considered more accurate and reliable than output from any individual model, as errors and natural variability from different models tend to offset each other (Pierce et al. 2009; Deser et al. 2012). To compare MACA and LOCA, eight models were chosen from each to represent the full range of uncertainties in future projections (Table 2). These models were chosen based on genealogy (Masson and Knutti 2011; Knutti et al. 2013), performance in simulating present-day climate over eastern North America and the Northeast (Sheffield et al. 2013; Miao et al. 2014; McSweeney et al. 2015; Karmalkar et al. 2019), global climate sensitivity (Miao et al. 2014), and climate sensitivity for the Northeast region (Table 2).

Data for both RCP4.5 and RCP8.5 scenarios are available from MACA and LOCA. While RCP8.5 was considered a high emission scenario, emissions and observed CO_2 concentration have closely tracked RCP8.5 over the past decade. Considering this recent trend and the climate security recommendation to build for a higher magnitude of warming than the target of international climate policy in case mitigation policies fail (Mabey et al. 2011; Sanford et al. 2014), this study makes use of the RCP8.5 scenario.

3. Precipitation indices and analysis method

To compare MACA and LOCA databases, we examine a variety of precipitation characteristics. A large array of indices have been proposed to quantify precipitation extremes (e.g., Frich et al. 2002; Zhang et al. 2011). While many of these indices have been widely used in climate change studies (e.g., Ahmed et al. 2013; Thibeault and Seth 2014), often only a subset of available climate indicators are used in any given climate change assessment. The choice of which indicators to include is often informed by assessment best practices and interactions with stakeholders to define decision needs and interests. In this study, based on core indices proposed by the joint CCl/CLIVAR/JCOMM Expert Team (ET) on Climate Change Detection and Indices (ETCCDI) (Karl et al. 1999) and considering stakeholder needs identified through the Connecticut state assessment (Seth et al. 2019; Kirchhoff et al. 2019), the following precipitation indicators are analyzed:

TABLE 1. Precipitation indices (as defined in section 3) over the area of Connecticut Regional Water Authority (RWA) reservoirs from different data sources.

Precipitation index	Amount (mm yr^{-1})	N_{wet} (days)	SII (mm day^{-1})	N_1inch (days)	CDD (days)	R1d (mm)	R5d (mm)
RWA rain gauges	1306	105	12.4	14.3	18	80	125
gridMET	1325	114	11.5	13.1	16.3	78	115
Livneh et al.	1314	160	8.2	7.8	15.7	55	114

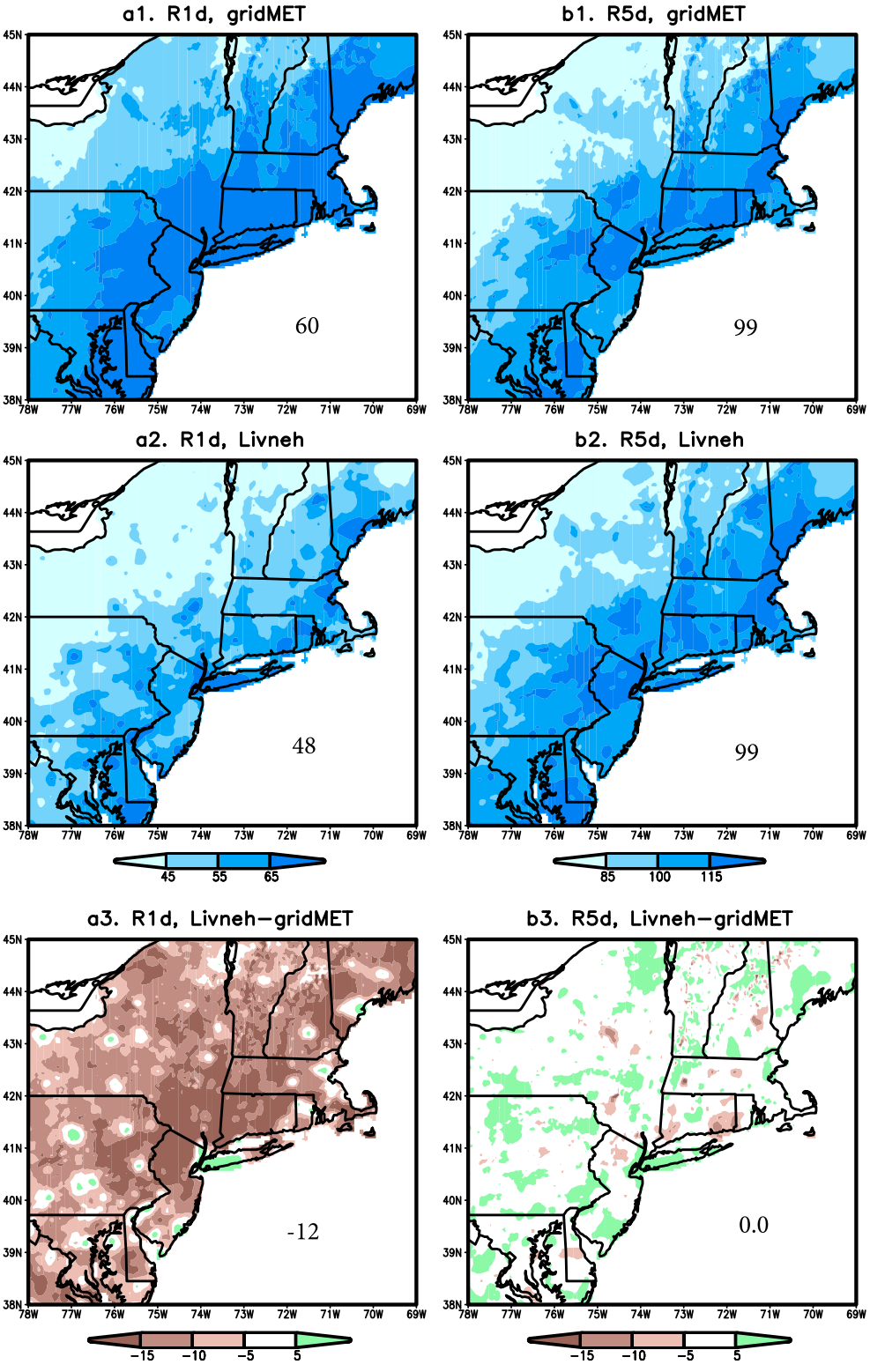

FIG. 2. The 34-year (1980–2013) average of annual 1-day maximum precipitation (R1d) and 5-day maximum precipitation (R5d), from gridMET and Livneh et al. and differences between the two products. The numbers written within each panel are spatial averages; units are millimeters.

AnnP, annual accumulation of precipitation amount;
N_wet, number of days (per year) with more than 1 mm of precipitation;
SII, simple intensity index (i.e., average amount of precipitation on each wet day);
CDD, maximum number of consecutive dry days for each JJA season;
N_1inch, number of days per year with more than 1 in. (25.4 mm) of precipitation;
P99, the 99th percentile of daily precipitation in the historical climate;
N99, number of days each year with precipitation exceeding the historical P99;
F99, fraction of annual precipitation accounted for by N99;
R1d, annual maximum 1-day precipitation;
R5d, annual maximum 5-day precipitation.

Note that in prior studies the maximum consecutive dry days (CDD) is typically defined for each year. However, in the U.S. Northeast, maximum CDD occurs during winter for most years, while summer (June–August) is the season of the highest water demand for agricultural and domestic usage. We therefore use the summer CDD for its regional relevance.

With the exception of P99 (which is estimated for the period 1970–99 only), all other metrics are estimated for each of the three 30-year periods, including historical 1970–99, midcentury 2040–69, and late century 2070–99; the multimodel ensemble mean of the projected changes by mid- and late century are analyzed. In addition, to support the development of climate adaptation strategies (e.g., revising infrastructure design criteria), the size of rare events (with a recurrence interval of N years) as well as the future recurrence interval of the past 1-in-N-years events are also estimated for R1d and R5d, with N equal to 5, 10, 20, 50, and 100, respectively. Despite of the challenges and uncertainties associated with the estimation of these extreme statistics, they are included here due to strong stakeholder interest and practical importance related to risk management.

The estimation of recurrence interval T of a given event size and the estimation of the event size X_N corresponding to a given recurrence interval N involves frequency analysis. This is done by fitting a theoretical distribution to the 30 years of data in each period for each model. For R1d and R5d, the generalized extreme value (GEV) distribution is chosen, and the L-moments method is used to estimate the location, scale, and shape parameters of the GEV distribution following previous studies (Hosking 1990; Kharin et al. 2013). These parameters are then used to estimate X_N for given recurrence interval N in different climates as well as the future recurrence interval T of the past extremes.

For most precipitation indices analyzed in this study, projected future changes are defined as the eight-model ensemble mean of the changes from the historical to midcentury and late century. An ensemble mean of changes at a given grid cell is estimated only if there is a high level of model consensus (defined as at least six out of the eight models agree) on the direction of projected changes, and the significance of the ensemble mean changes is tested using a one-sided t test with $\alpha = 0.05$. Changes for which the degree of model consensus is low or the magnitude of the ensemble mean does not pass the significance test are considered inconclusive, and are excluded from both the spatial distribution plotting and domain averaging.

4. Results

a. Observations and model historical climate

The observational data underlying the two databases, gridMET and Livneh et al. (2015), are similar in temporally aggregated precipitation but differ significantly in the day-to-day variation of precipitation (Fig. 1), leading to significant differences in most of the precipitation indicators examined in this study. As the objective of a statistical downscaling method for the historical period is to reproduce the statistics of the training data, not surprisingly, the historical eight-model ensemble mean of downscaled precipitation characteristics from MACA and LOCA (Figs. 3–5) are almost identical to those from the gridMET and Livneh et al. data, respectively, and differ significantly between MACA and LOCA. For each database, slight differences between the downscaled model climates and the training data can be attributed to decadal variability and model internal variability. The following description of historical climate therefore focuses on the comparison of model climate between LOCA and MACA (Figs. 3–5), with the understanding that these mostly reflect the differences between the two training datasets.

The annual precipitation climatology for LOCA and MACA during the historical period closely resemble each other in spatial pattern (Fig. 3). This is expected due to the agreement between the two training datasets in annual precipitation, both of which were adjusted to reproduce PRISM (Daly et al. 1994). The domain average of annual precipitation is slightly lower in LOCA (1097 mm yr^{-1}) than in MACA (1146 mm yr^{-1}) (Table 3). The 30-year average of daily precipitation characteristics based on the eight-model ensemble mean substantially differs between the two databases. Across the domain of analysis, heavy precipitation is less frequent and less intense in LOCA than in MACA (as reflected by N_1inch, F99, R1d) (Figs. 3 and 4), which is consistent with the general underestimation of heavy precipitation in LOCA's training data. Relative to MACA, a similar amount of precipitation in LOCA is distributed among a larger number of wet days, leading to a lower mean intensity, with SII spatially averaged to 7.1 mm day^{-1} in LOCA and 8.7 mm day^{-1} in MACA (Table 3 and Fig. 3). There are fewer heavy precipitation days in LOCA than in MACA (Fig. 4), with a spatial average of N_1inch at ~4.4 days compared to 8 days. Extremely heavy precipitation (defined as events exceeding the 99th percentile of daily precipitation) accounts for a lower fraction of annual precipitation in LOCA, with a spatial average of 11.6% for F99 (compared to 14.2% in MACA) (Fig. 4). The annual maximum 1-day precipitation is also significantly lower in LOCA, averaging to 45 mm (compared to 58 mm in MACA) (Fig. 5). For all these precipitation metrics, despite the differences in magnitude, LOCA and MACA demonstrate a similar spatial pattern, which (with the exception of N_wet) features an increase from

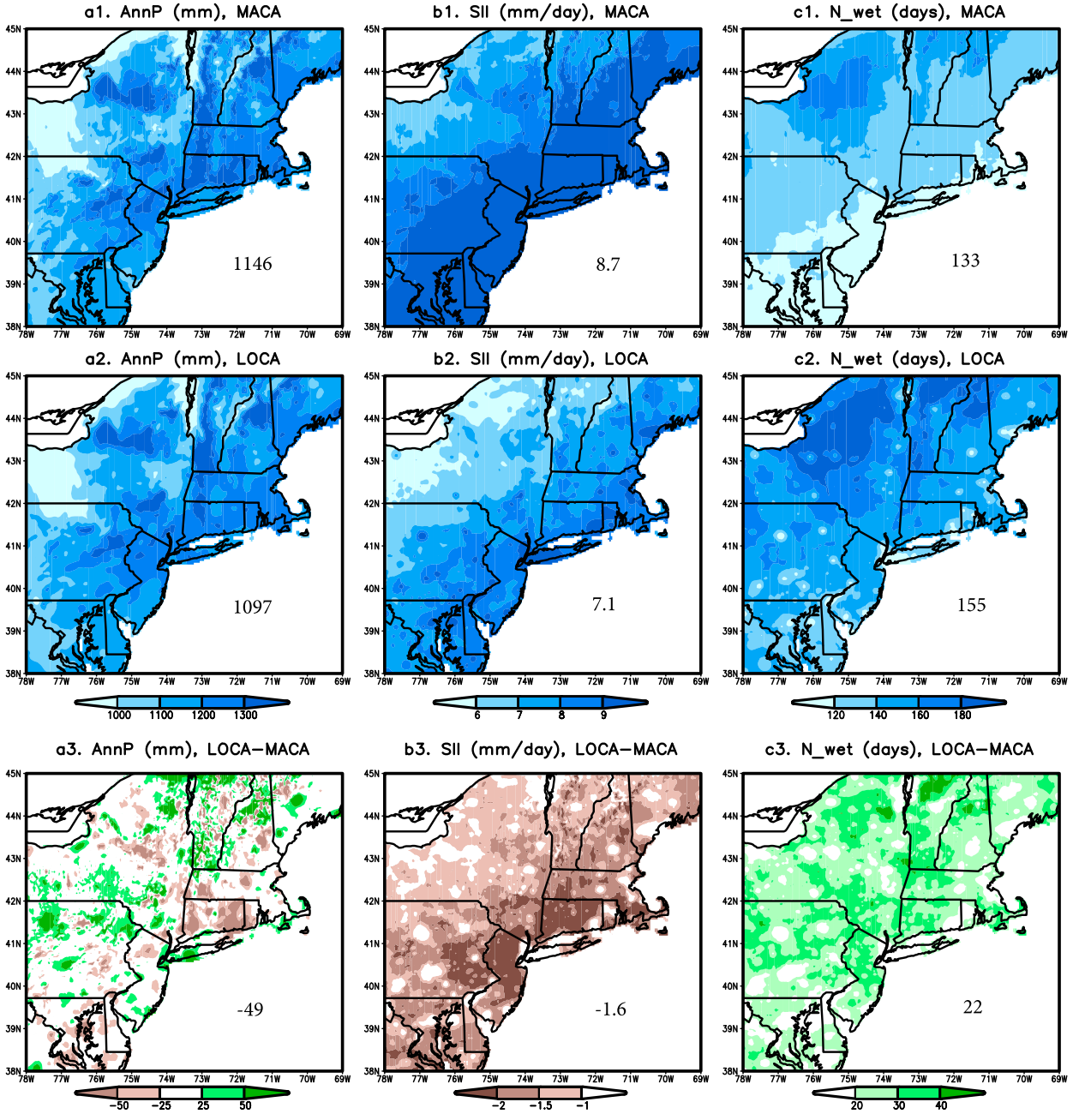

FIG. 3. Eight-model ensemble mean for the 30-year average of annual precipitation (AnnP), simple intensity index (SII), and the annual wet days (N_wet) during the historical period (1970–99), from MACA and LOCA, and differences between the two. The numbers written within each panel are spatial averages.

inland toward the coastal region and from low elevation to high elevation.

In the Northeast, most of the rare and extremely rare precipitation events are related to tropical storms/hurricanes in late summer and fall as well as nor'easters during winter. The sizes of daily precipitation with a recurrence interval of 20 and 100 years, respectively, are presented in Fig. 5. Consistent with other daily precipitation characteristics, the magnitude of the 1-day precipitation during these rare events is much smaller in LOCA than in MACA. In LOCA, precipitation during these rare events follows a spatial pattern similar to the average events, with a general coast–inland contrast; in MACA, the large-scale spatial pattern of precipitation during these rare events deviates from the average events, with a northeast–southwest–oriented heavy precipitation band slightly inland away from the coast. Both products show a clear topographic fingerprint of rare daily precipitation, with local maxima over the ridgeline of the

TABLE 2. The eight global models included in the analysis, development groups, global temperature sensitivity under RCP8.5, Northeast (NE) annual temperature and precipitation changes (ΔT and ΔP) between reference (1970–99) and midcentury (2040–69) under RCP8.5, and model biases over eastern North America (ENA) for simulating summer (JJA) temperature and precipitation.

Model name	Development group	Time to global +2.0°C over preindustrial	NE ΔT (°C)	NE ΔP (mm)	Model biases over ENA for JJA T (°C) and P (%)
CanESM2	CCMA (Canada)	2030 (high)	+3.7	+86	3.1°C, −22.2%
HadGEM2-CC	Met Office (United Kingdom)	2032 (high)	+4.4	+134	1.0°C, −0.04%
IPSL-5A-LR	IPSL (France)	2042 (medium)	+3.3	+59	0.4°C, 9.9%
CCSM4	NCAR (United States)	2043 (medium)	+2.7	+115	1.2°C, 7.7%
CSIRO-Mk3.6.0	CSIRO (Australia)	2045 (medium)	+3.2	+150	1.3°C, −17.3%
GFDL-ESM2M	GFDL (United States)	2049 (low)	+2.3	+89	−0.3°C, −5.2%
BCC-CSM1.1	BCC (China)	2052 (low)	+3.2	+120	0.16°C, −20.6%
INMcm4	INM (Russia)	2060 (low)	+1.9	+4	−1.7°C, 17.9%

Catskill (New York), Green (Vermont), and White (New Hampshire and Maine) Mountains.

In summary, for historical climate, MACA and LOCA are similar in precipitation amount, but differ substantially in the mean and extremes of daily precipitation characteristics. These differences are mostly attributed to the underlying observational datasets, and do not reflect differences in the downscaling method.

b. *Projected future changes*

1) CHANGES IN PRECIPITATION AMOUNT

Results from the two products show remarkably similar spatial pattern of projected changes in precipitation with stronger increases over high altitudes than valleys, based on the absolute changes (e.g., Figs. 6a1–a4); relative changes in both products show little spatial variation (results not shown). Table 3 lists the spatial average of annual and seasonal precipitation and projected changes for midcentury and late century, based on the eight-model ensemble mean. Despite some differences in the absolute amount, MACA and LOCA agree well in projecting the relative changes. For example, the annual total precipitation is projected to increase 7%–8% by midcentury (2040–69) and approximately 10.5% by late century in both products. These projected increases are due primarily to increases in the winter and spring seasons. In both products, there is a high degree of model consensus across the whole domain in projecting a significant increase of precipitation in winter and spring for both future periods. For summer precipitation over most of the domain, the degree of model consensus on an increase is high for midcentury and low for late century, suggesting a higher degree of uncertainty for warm-season precipitation projections further into the future. For fall precipitation during both future periods and in both products, the eight models either disagree on the direction of changes or project changes that are statistically not significant.

2) CHANGES IN PRECIPITATION CHARACTERISTICS AND EXTREMES

For projected future changes of precipitation characteristics (with the exception of annual maximum 1-day precipitation), results from LOCA and MACA are generally similar despite their significant differences in the historical climate. According to both products, changes in N_wet and summertime CDD are inconclusive for both future periods. Over most of the domain the level of model consensus is low on the direction of changes; over the small fraction of the region where the degree of model consensus is high, summer CDD is projected to increase by both LOCA and MACA while N_wet is projected to increase in MACA and decrease in LOCA (Figs. 6c1–c4 and 7a1–a4). For SII, N_1inch, and F99, both LOCA and MACA project significant increases with a high degree of model consensus, and their absolute changes are very similar between the two products especially for the late century (Figs. 6b1–b4 and 7b1–c4). For the midcentury period, MACA projects slightly larger increases than LOCA; the increase continues beyond midcentury, but at a slower pace in MACA than in LOCA, arriving at a similar magnitude of total changes in the two products by the late century. For all these three metrics (SII, N_1inch, and F99), historical reference is substantially lower in LOCA than in MACA. As such, similar absolute changes translate to a larger relative change in LOCA than in MACA (Table 4).

The projected changes in the long-term mean of annual maximum 1-day precipitation (R1d) differ significantly between the two products, with LOCA projecting a much smaller increase than MACA for both future time periods. This statement holds for both the absolute and relative changes (Fig. 8), and the differences between LOCA and MACA are larger in magnitude than the standard deviation among the eight GCMs (Table 4). MACA projects a faster increase from the historical period to midcentury than LOCA and a slower increase from midcentury to late century. Despite the substantial differences in magnitude, the spatial pattern of projected future changes is similar between the two products, with the strongest changes along the Northeast corridor and the east coast of New England. There is a high degree of model consensus on the increase of average R1d across the domain in MACA and over most of the domain in LOCA; there are scattered small areas in LOCA where the degree of model consensus in projecting the direction of changes is very low.

Relative to the projected changes in the multiyear mean of R1d, the differences between LOCA and MACA in projecting R1d changes during rare extremes (e.g., R1d_20, or 1-in-20-years events) are larger (Fig. 8); within each product, differences

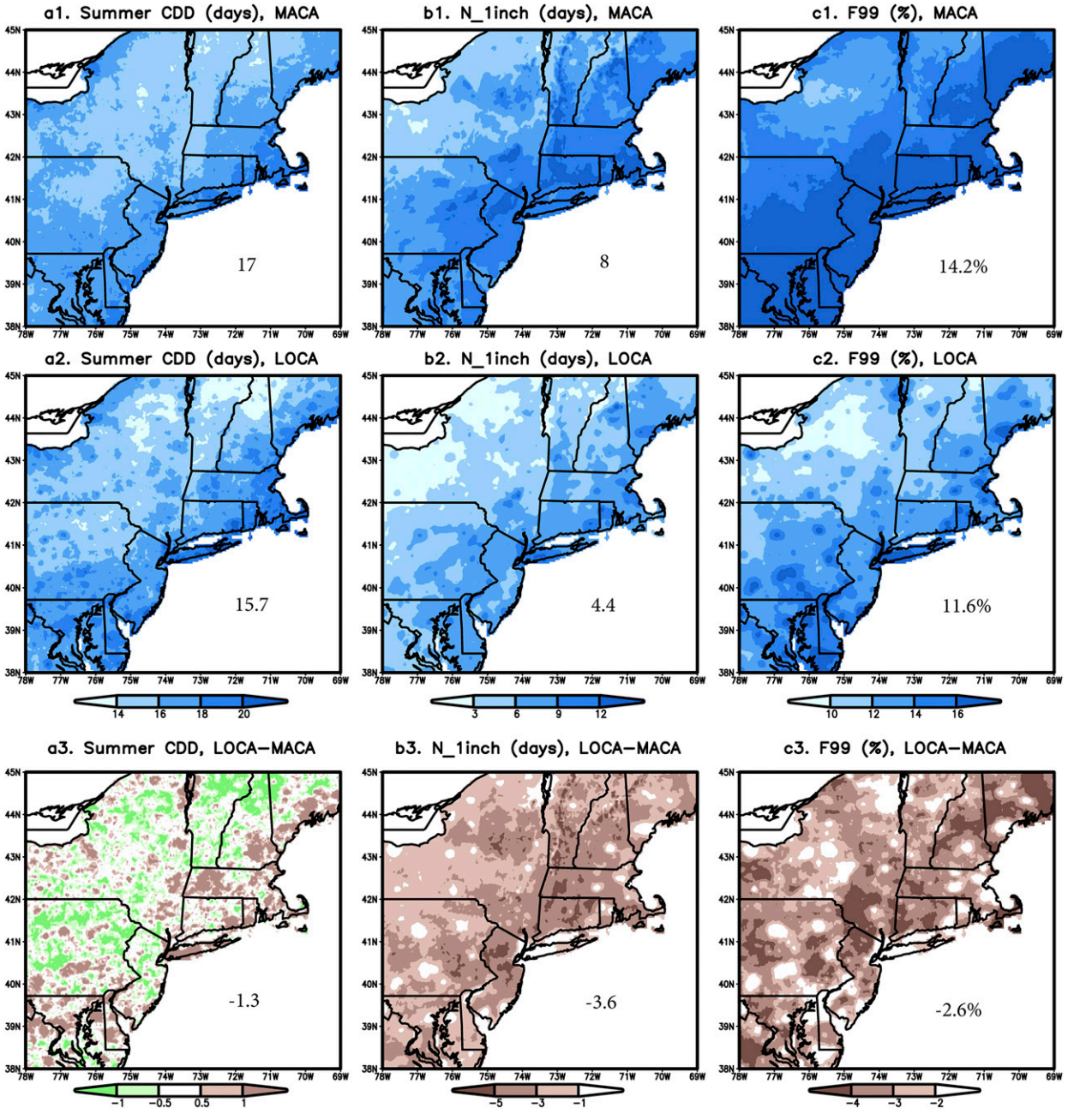

FIG. 4. Eight-model ensemble mean for the 30-year average of maximum consecutive dry days (summer, CDD), annual total number of days with more than 1 in. of precipitation (N_1inch), and the fraction of total precipitation accounted for by extreme events with daily precipitation exceeding the 99th percentile (F99), from MACA and LOCA, and differences between the two. The numbers written within each panel are spatial averages.

among models are larger too, leading to a lower level of model consensus in projecting the direction of changes of rare extremes than the R1d mean (Fig. 8). Results for other recurrence intervals are qualitatively similar. MACA projects a strong increase of the intensity of R1d_20 with a high degree of model consensus over most of the domain; for rarer evens (e.g., 1-in-100-years, results not shown), the areas are larger where projected changes are inconclusive. Over areas of strong model consensus, MACA projects larger increases of precipitation during rare events for midcentury than for late century (e.g., 43% versus 31% for R1d_20). While this is counter intuitive, it is consistent with the slowdown of the average R1d increase from midcentury to late century, and likely results from extra processing in the MACA approach such as epoch removal and replacement (Wootten 2018). Strong model consensus in projecting future precipitation changes in rare events in LOCA is limited to a much smaller

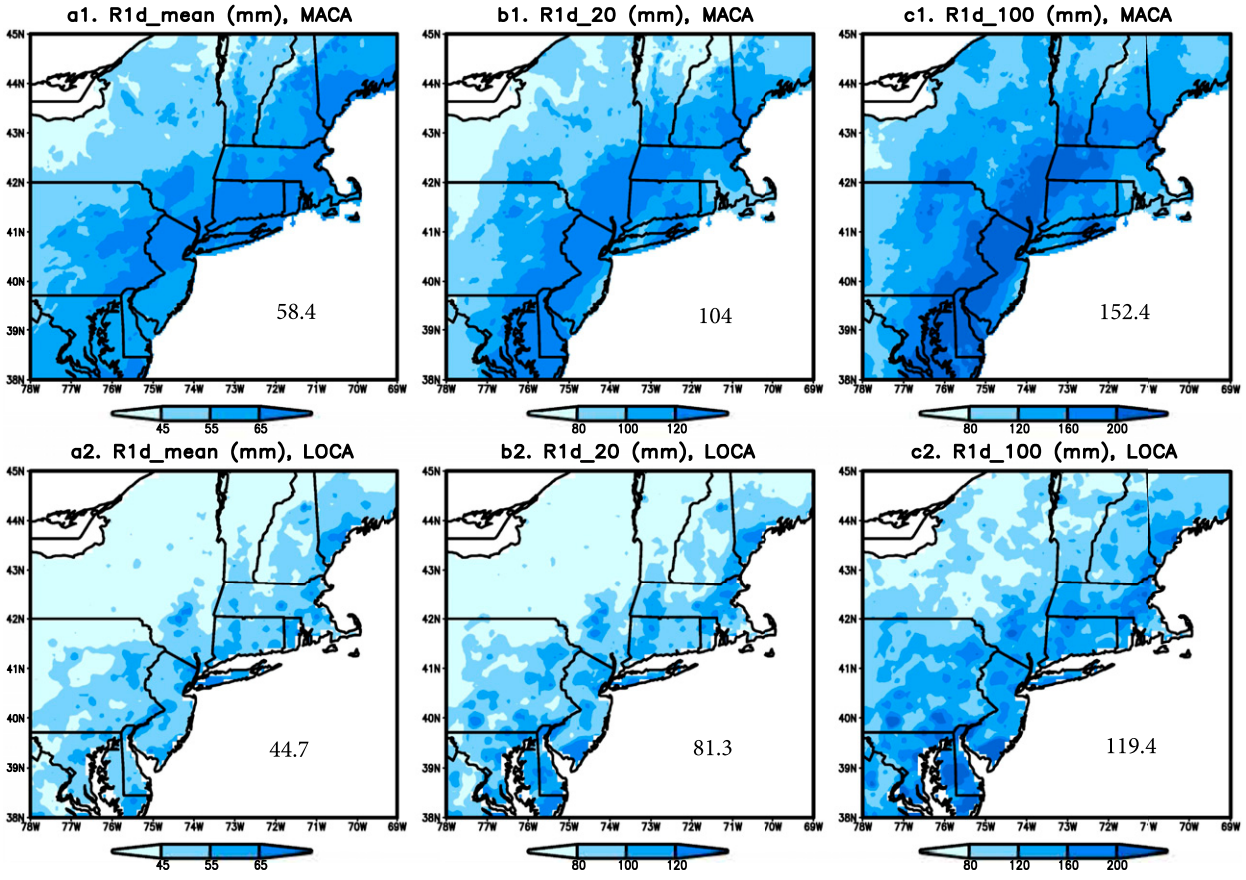

FIG. 5. The eight-model ensemble mean of 1-day maximum precipitation corresponding to the 30-year average (R1d_mean), extreme events with a recurrence interval of 20 and 100 years (R1d_20 and R1d_100), respectively, defined for the reference period 1970–99 based on MACA and LOCA. The numbers written within each panel are spatial averages.

portion of the domain than in MACA; however, where there is a strong model consensus, an increase is projected. Different from MACA, the magnitude of projected changes in LOCA continues to increase from midcentury to late century. For the changes from historical to late century, the difference between LOCA and MACA is small in projecting the relative changes of R1d mean and R1d_20. The greatest differences between LOCA and MACA (and the counter intuitive comparison between midcentury and late century in MACA) are related to a very strong increase of annual maximum 1-day precipitation from historical to midcentury in the MACA database. By midcentury, the absolute increase projected by MACA is a factor of 2 higher than that projected by LOCA for the mean R1d, and a factor of 3 for R1d_20; the relative changes in MACA are a factor of 2 higher for both R1d and R1d_20. These differences get attenuated by late century.

MACA and LOCA differ substantially in projecting the frequency of major precipitation events (Fig. 8). In MACA, the

TABLE 3. Eight-model ensemble of precipitation climatology (mm) during the historical period and the projected changes from historical reference to midcentury and late century, averaged over the Northeast. The ensemble is presented as $\mu \pm \sigma$, where μ is the mean and σ is the standard deviation among the eight models. Percentage values in parentheses are relative changes. A dash "—" indicates a low degree of model consensus regarding the direction of changes and/or lack of statistical significance. Note that all changes are positive (i.e., precipitation increase).

	1970–99 reference		2040–69 changes		2070–99 changes	
Variables	MACA	LOCA	MACA	LOCA	MACA	LOCA
Annual total	1146 ± 10	1097 ± 12	95 ± 44 (8.3%)	83 ± 44 (7.6%)	120 ± 61 (10.5%)	116 ± 54 (10.6%)
Winter (DJF)	238 ± 6	242 ± 4	35 ± 24 (14.7%)	36 ± 24 (14.9%)	47 ± 23 (19.7%)	45 ± 21 (18.6%)
Spring (MAM)	289 ± 5	274 ± 6	29 ± 18 (10.0%)	26 ± 16 (9.5%)	51 ± 12 (17.6%)	51 ± 14 (18.6%)
Summer (JJA)	308 ± 7	293 ± 6	21 ± 14 (6.8%)	19 ± 12 (6.5%)	—	—
Fall (SON)	311 ± 9	289 ± 7	—	—	—	—

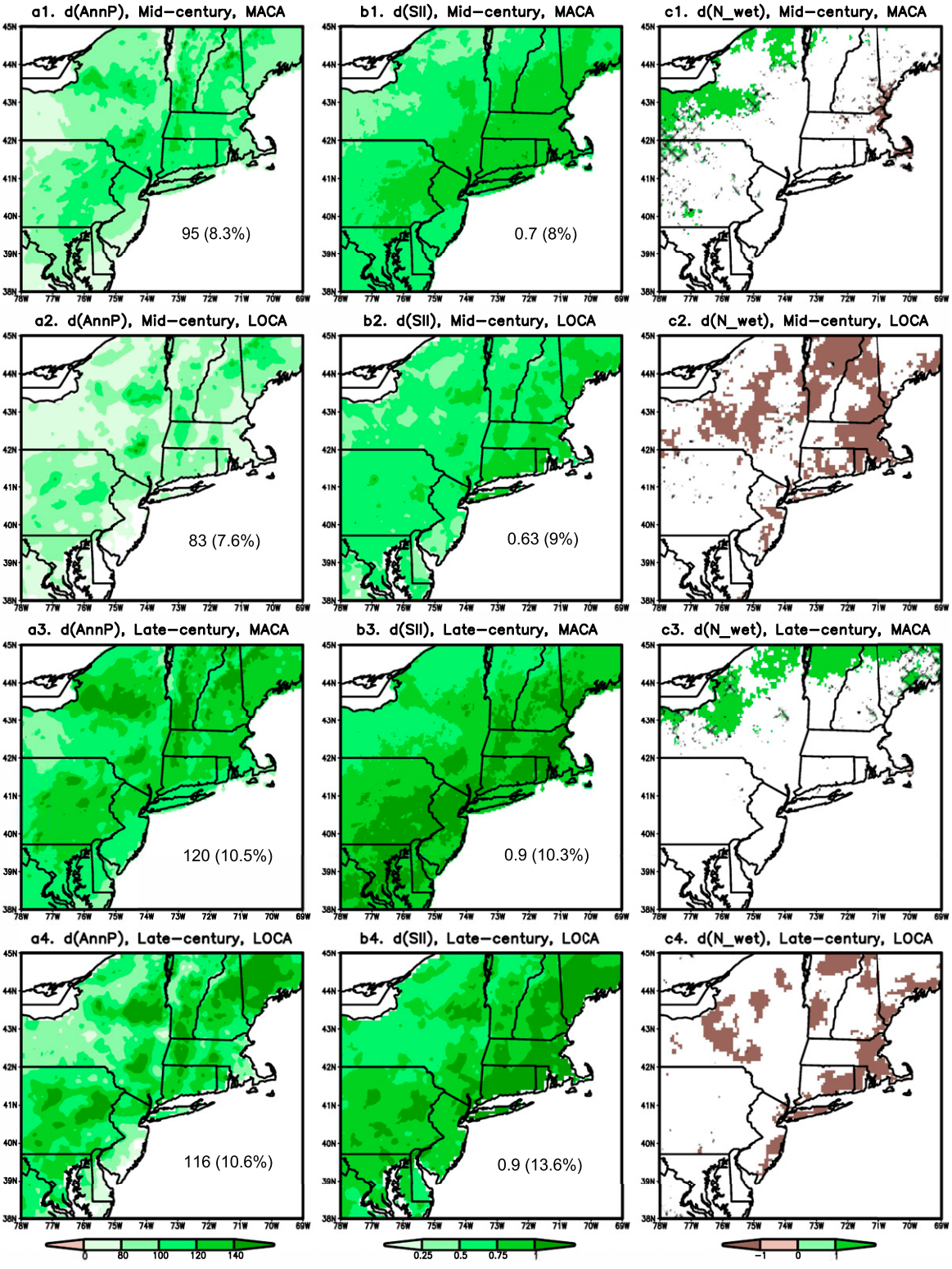

FIG. 6. The eight-model ensemble mean of projected future changes for annual precipitation d(AnnP) (mm), simple intensity index d(SII) (mm day^{-1}), and annual wet days d(N_wet) (days) by the midcentury and late century, based on MACA and LOCA. White areas over land (with no shading) indicate a lack of model consensus on the direction of projected changes (i.e., the 8 models split 4-to-4 or 5-to-3); black hatching indicates changes that are statistically not significant. The numbers written within each panel are spatial averages where model consensus exists over a substantial portion of the domain.

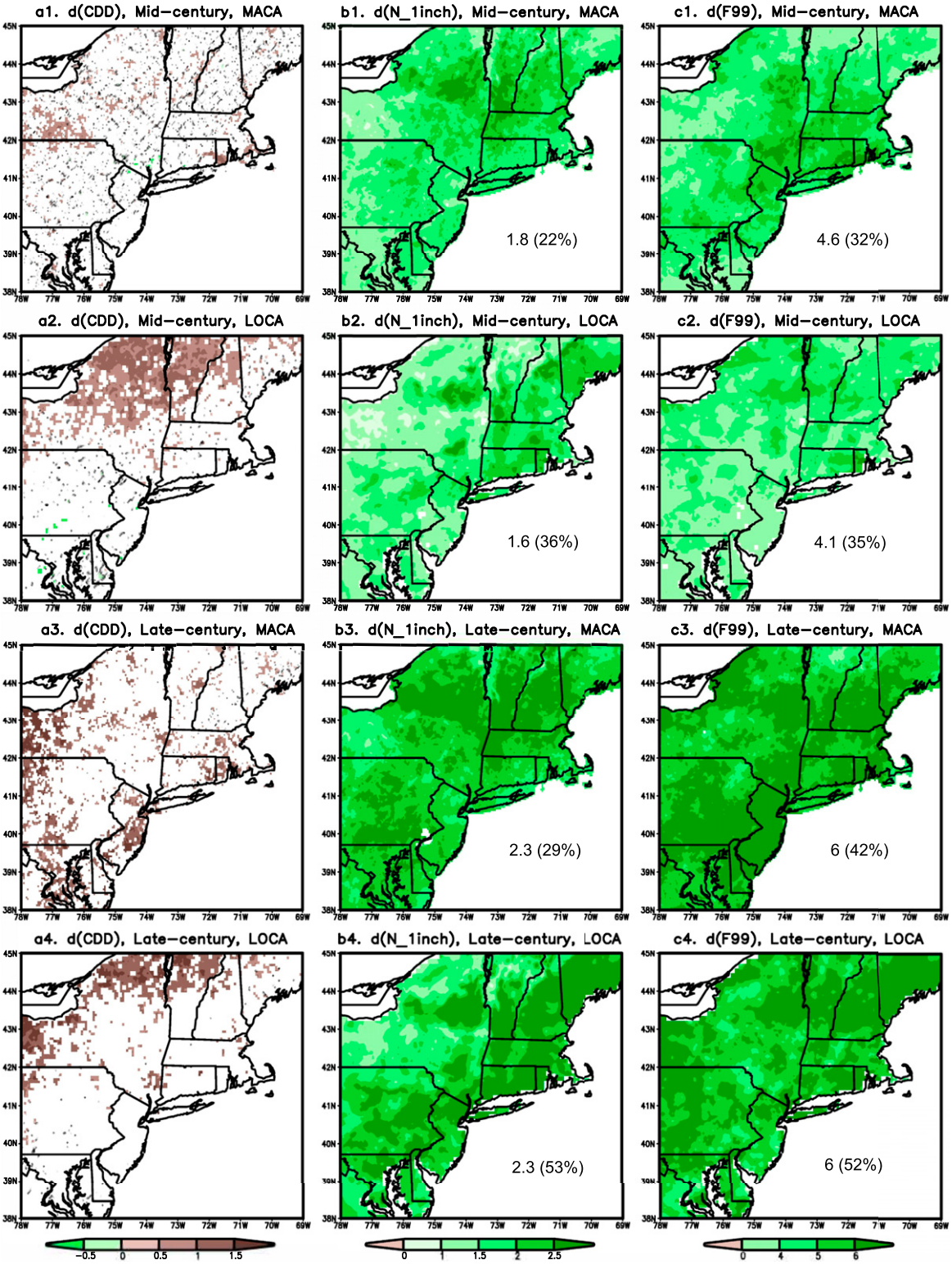

FIG. 7. The eight-model ensemble mean of projected future changes for consecutive dry days in summer "*d*(CDD)," annual total number of days with more than 1 in. of precipitation "*d*(N_1inch)," and the fraction of total precipitation accounted for by extreme events with daily precipitation exceeding the 99th percentile "*d*(F99)" by the midcentury and late century, based on MACA and LOCA. White areas over land (with no shading) indicate a lack of model consensus on the direction of projected changes (i.e., the 8 models split 4-to-4 or 5-to-3); black hatching indicates changes that are statistically not significant. The numbers written within each panel are spatial averages where model consensus exists over a substantial portion of the domain.

TABLE 4. Eight-model ensemble of precipitation metrics on intensity and extremes during the reference period and the projected changes from historical reference to midcentury and late century, averaged over the Northeast. The ensemble is presented as $\mu \pm \sigma$, where μ is the eight-model mean and σ is the standard deviation among the eight models. All changes are positive (i.e., increases). Percentage values in parentheses are changes relative to reference.

	1970–99 reference		2040–69 changes		2070–99 changes	
Metrics	MACA	LOCA	MACA	LOCA	MACA	LOCA
SII (mm day^{-1})	8.7 ± 0.06	7.1 ± 0.06	0.7 ± 0.27 (8%)	0.63 ± 0.34 (9%)	0.9 ± 0.47 (10.3%)	0.9 ± 0.53 (13.6%)
N_1inch (days)	8 ± 0.19	4.4 ± 0.15	1.8 ± 0.8 (22%)	1.6 ± 0.8 (36%)	2.3 ± 1.3 (29%)	2.3 ± 1.1 (53%)
F99 (%)	14.2 ± 0.2	11.6 ± 0.1	4.6 ± 1.9 (32%)	4.1 ± 2.0 (35%)	6 ± 2.8 (42%)	6 ± 2.7 (52%)
R1d_mean (mm)	58 ± 0.9	45.1 ± 0.7	12 ± 3.7 (21%)	5.8 ± 2.7 (13%)	13 ± 4.2 (22%)	8.3 ± 3.1 (18%)
R1d_20yrs (mm)	104 ± 5.6	82.6 ± 2.6	43 ± 17 (41%)	13.4 ± 5 (16%)	31 ± 13 (30%)	19 ± 8.5 (23%)

historical 1-in-20-years 1-day precipitation events are projected to occur every 5–10 years over most of the region in mid- and late century. In LOCA, strong model consensus on projecting more frequent occurrence of the previously 1-in-20-years events is limited to a much smaller fraction of the domain than in MACA; over a large portion of the region, previously rare events are projected to become even less frequent. In both products, the projection for rarer events (e.g., 1-in-100-years) is subject to a higher degree of uncertainty.

Using three metropolitan areas (Boston, New York City, and Washington, D.C.) as examples, Fig. 9 compares the statistical distribution of the spatially averaged, annual maximum 1-day precipitation of LOCA and MACA based on the quantile–quantile (Q–Q) analysis. These Q–Q plots effectively summarize the heavy precipitation comparisons between the two products and between past and future climates. From low quantiles to high quantiles, the different lines of the same color increasingly diverge, reflecting an increasing degree of model uncertainty (or intermodel variation); despite of the model uncertainties, the signal is clear that R1d is generally lower in LOCA than in MACA (with most of the lines below the 1:1 line), and their differences (as reflected by the deviation from the 1:1 line) increases from low quantiles (common events) to high quantiles (rare events) and from historical to future climates. While R1d in both future periods is clearly higher than the historical reference, the differences between the two future periods are small and subject to a great degree of model uncertainty.

c. *Potential causes for the differences between LOCA and MACA*

The most substantial differences between LOCA and MACA in future projections are in the changes of annual maximum 1-day precipitation. The downscaling approach, the training data, and their interplay contribute to the differences between LOCA and MACA. Using individual models as an example, Table 5 compares the spatial averages of the historical reference, projected future changes from historical to midcentury and late century among LOCA, MACA-L, and MACA. Note that LOCA and MACA-L use the same training data but differ in downscaling method; MACA-L and MACA were produced using the same downscaling approach but different training datasets. During the historical period, the mean R1d in MACA-L is larger than in LOCA, which is a result of both a slight difference in the specific time period of the Livneh et al. data used as training and differences between the downscaling methods; the mean R1d in MACA is the highest, which is expected based on the high R1d values in the training data (gridMET, Fig. 2). The projected changes are quite close between MACA-L and MACA, but differ significantly between LOCA and MACA-L. This suggests differences in the projected changes are primarily caused by differences of the downscaling method, rather than the training data used. For any given GCM (GFDL or CCSM4), the projected R1d changes by the late century are larger than by the midcentury over most of the domain in LOCA, over about half of the domain in MACA-L, and over a small fraction of the domain in MACA (results not shown). From the historical period to midcentury, R1d is projected to increase much faster in MACA-L and MACA (~20%) than in LOCA (~10%); the increase beyond midcentury continues in LOCA but slows down or stalls in MACA-L and MACA (Table 5). This statement holds qualitatively for the downscaled products of all individual GCMs, although the spatial pattern and magnitude of the projected changes differ among them.

To understand the large differences between LOCA and MACA in projecting changes for the midcentury, comparison with the raw GCM output was conducted. Using CCSM4 as an example, Fig. 10 compares the historical R1d and projected midcentury changes derived from the GCM, LOCA, and MACA. Note that the similarity of the R1d magnitude between LOCA and the GCM is a coincidence: LOCA underestimates R1d due to the underestimation in its training data, while the GCM underestimates R1d due to its coarse resolution. The similarity between LOCA and the GCM in the projected relative changes, both in terms of the magnitude and large-scale spatial pattern, is by design. The LOCA downscaling method attempts to preserve the GCM-predicted relative change evaluated as a percent of the GCM's historical climatology, and applies the GCM-derived percent change to the training data to derive the future values. This intentional preservation of relative change together with the (coincidental) CCSM4-LOCA similarity in historical statistics lead to the CCSM4-LOCA similarity in the projected absolute changes. The MACA algorithm includes a similar design for preserving relative changes, but was implemented at a different time scale (monthly, as opposed to yearly in LOCA) to improve the precipitation seasonal cycle. As such, in MACA, the relative

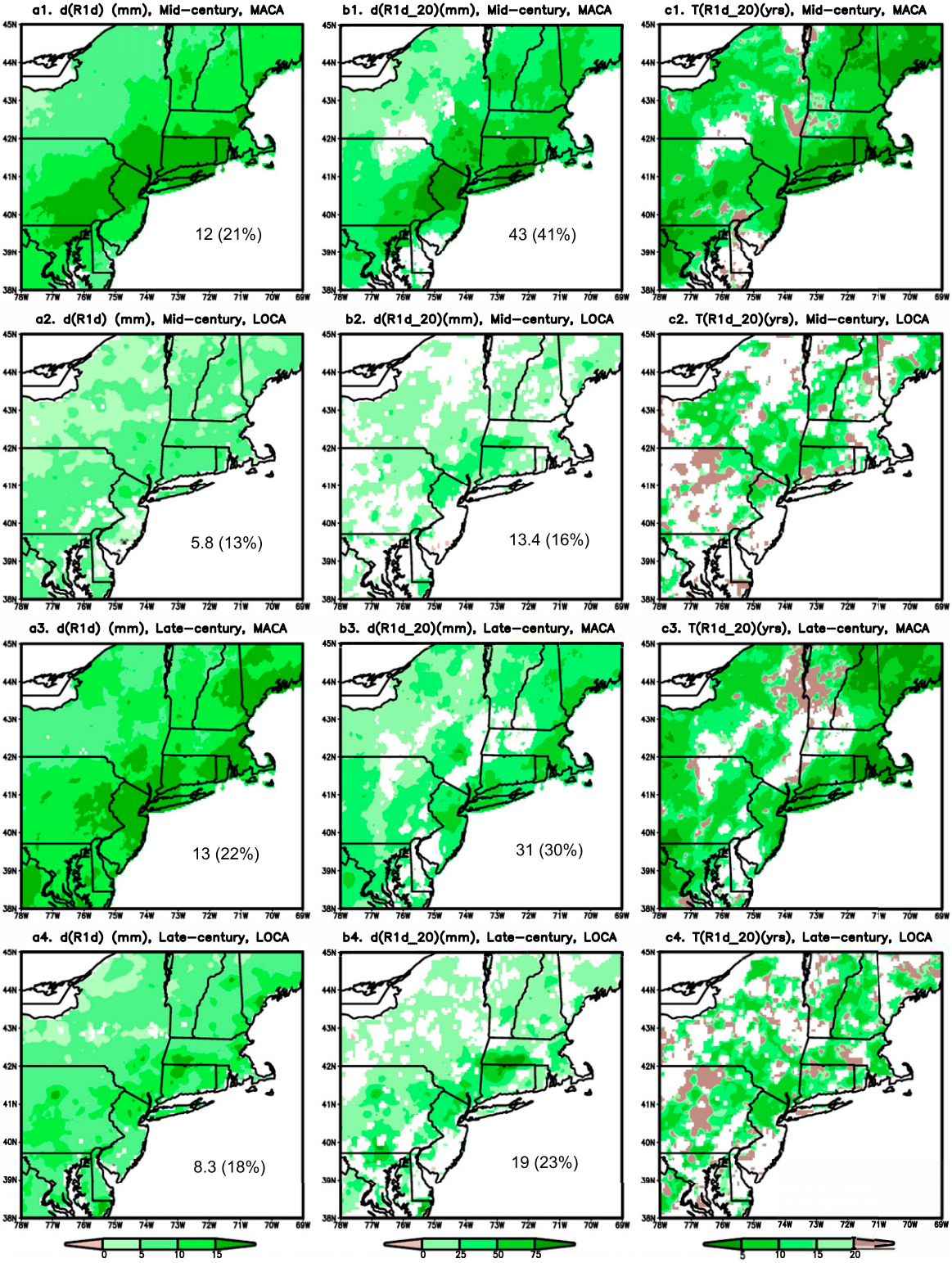

FIG. 8. The eight-model ensemble mean of projected future changes in the 30-year mean of (left) 1-day maximum precipitation "*d*(R1d)" and (center) 1-day maximum precipitation with a recurrence interval of 20 years "*d*(R1d_20)," by the midcentury and late century based on MACA and LOCA; (right) future recurrence interval of events that occurred once every 20 years during the historical period. The lack of shading over land indicates a lack of model consensus (i.e., the 8 models split 4-to-4 or 5-to-3) on whether the change is an increase or decrease, or on whether the future recurrence interval is expected to be longer or shorter than 20 years; black hatching (if present) indicates changes that are statistically not significant. The numbers written within each panel are spatial averages where model consensus exists over a substantial portion of the domain and where spatial averaging is meaningful.

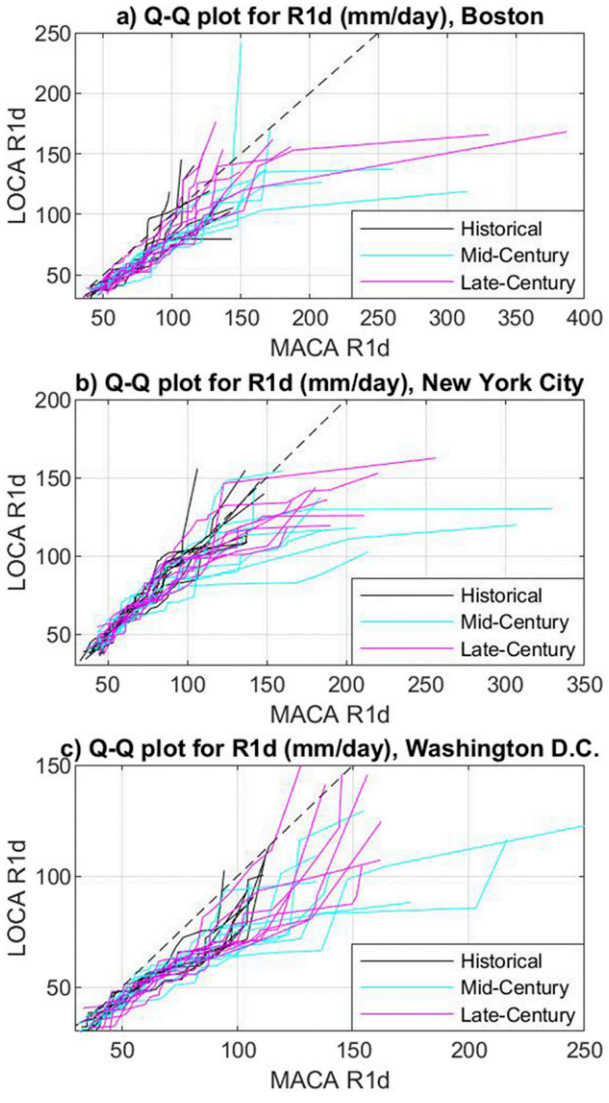

FIG. 9. The eight-model ensemble of Q–Q plot for the annual maximum 1-day precipitation (R1d; mm day^{-1}) between LOCA and MACA in historical, midcentury, and late-century climates, for three metropolitan areas: (a) Boston, (b) New York City, and (c) Washington, D.C. Each solid line represents one model, and the 1:1 line is dashed.

changes from the GCM were preserved for the monthly mean but not for the annual maximum 1-day precipitation. MACA starts with a much higher historical R1d (due to the more realistic training data gridMET), and also projects a much larger (absolute and relative) increase of mean R1d than LOCA. The projected increase in MACA follows a large-scale spatial pattern similar to the historical mean (and bears more similarity to the observed distribution of precipitation extremes), leading to a ''heavy-becomes-heavier'' scenario. The spatial pattern of precipitation and precipitation extremes from GCMs often deviate from observations, as evident from Fig. 10. The analog approach corrects these spatial biases by taking the weighted average of precipitation observed on days with similar large-scale features as the day to be downscaled. This, together with the bias correction procedure, causes the differences between the GCM and the downscaled products in the spatial pattern of projected changes.

5. Summary and discussion

Statistically downscaled climate databases are often used in climate change assessments to inform climate adaptation efforts without much attention to how the choice of dataset may influence assessment findings. In this study, future changes of precipitation and precipitation extremes in the U.S. Northeast are assessed based on two statistically downscaled climate databases with fine spatial resolution and results are compared. A special focus of this study is on interrogating the similarity and differences between the two databases, MACA and LOCA, and on identifying potential causes for differences. Future changes are defined with respect to the historical reference period of 1970–99, for the midcentury (2040–69) and late century (2070–99) corresponding to the RCP8.5 scenario based on the ensemble of eight models. The main findings are summarized as follows:

1) Both MACA and LOCA project significant annual precipitation increases, and the projected changes are similar in magnitude, spatial pattern, and seasonality. The largest increases of precipitation are projected during winter and spring, with smaller increases during summer and inconclusive changes during autumn due to the lack of model consensus on the direction of changes.
2) Both MACA and LOCA project significant increases of several precipitation intensity metrics across the region with strong model consensus, including the number of days with more than one inch of precipitation, the simple intensity index, and the fractional of annual precipitation accounted for by days of heavy precipitation (exceeding the 99th percentile of daily precipitation). The two products are similar in the magnitude of absolute changes, but the relative changes are larger in LOCA due to underestimation of heavy precipitation intensity metrics in LOCA's training data.

TABLE 5. The domain average of 30-year mean of maximum 1-day precipitation "R1d" (mm day^{-1}) for the historical period and the projected changes for midcentury and late century (relative to historical reference), based on LOCA, MACA-L, and MACA for GFDL and CCSM4.

	GFDL			CCSM		
Datasets	Historical reference	Midcentury changes	Late-century changes	Historical	Midcentury changes	Late-century changes
LOCA	45	5.5 (12%)	9.6 (21%)	45.5	4.6 (10%)	6.5 (14%)
MACA-L	51.2	9.9 (19%)	11.4 (22%)	50	9.5 (19%)	10.9 (22%)
MACA	58.5	11 (19%)	10.4 (18%)	57.5	11.6 (20%)	12.9 (22%)

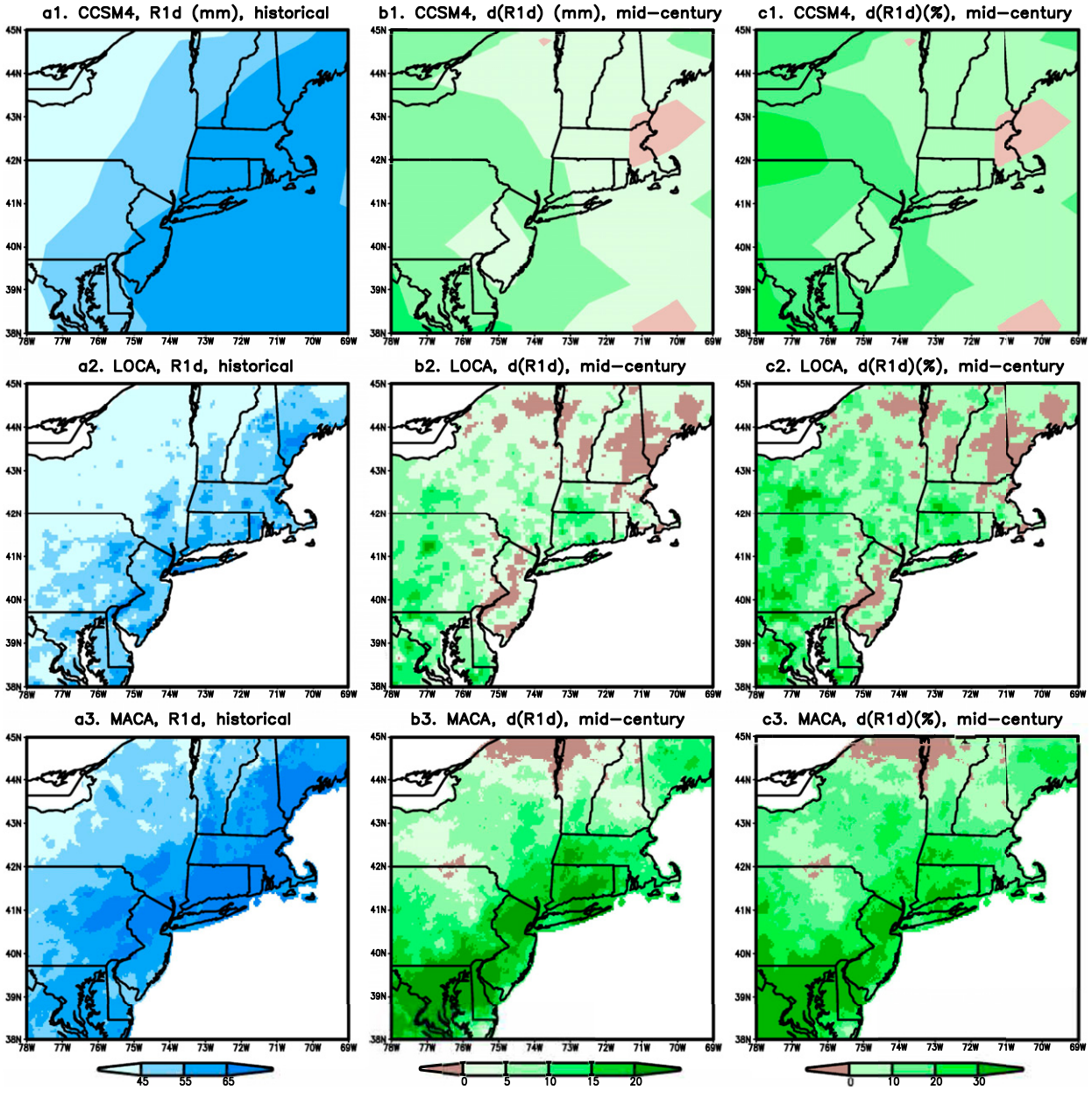

FIG. 10. (left) The 30-year average of 1-day maximum precipitation "R1d" during the historical period and projected (center) absolute changes and (right) relative changes "*d*(R1d)" by midcentury, based on (top) CCSM4 output and the corresponding downscaled data from (middle) LOCA and (bottom) MACA.

3) Both MACA and LOCA project significant increases in the long-term mean of annual maximum 1-day precipitation across the region and with a high degree of model consensus. The magnitude of both the absolute and relative changes in maximum 1-day precipitation are smaller in LOCA than in MACA, due to differences in both the downscaling method and training data.
4) MACA and LOCA show major differences in projecting changes to the rare 1-day precipitation (e.g., 1-in-20-years). In MACA, both the intensity and frequency of rare events are projected to significantly increase, with a high degree of model consensus across most of the domain. In LOCA, model consensus is lacking over most of the domain; where models do agree, the projected changes have a smaller magnitude than in MACA.
5) In MACA, the annual maximum 1-day precipitation is projected to increase swiftly from present day to midcentury, and then increase more slowly from the midcentury to late century; in contrast, the projected trend of the maximum 1-day precipitation in LOCA is approximately linear.

Despite differences between MACA and LOCA in both the downscaling methodology and training data used, the projected future changes of precipitation and precipitation extremes from the two products are qualitatively similar for the most part. The increase of precipitation amount and the increase of heavy precipitation frequency and intensity found in both products are qualitatively consistent with results from many previous studies on trend and changes over the U.S. Northeast (e.g., Keim and Rock 2002; Groisman et al. 2004, 2005; Griffiths and Bradley 2007; Brown et al. 2010; Hodgkins and Dudley 2011; Kunkel et al. 2013; Janssen et al. 2014; Walsh et al. 2014; Thibeault and Seth 2014; Easterling et al. 2017). For climate assessments in terms of informing the general direction of local climate adaptation for flood risks, either one of the two products is appropriate. However, quantitatively, the specific magnitude of these increases (especially of those related to extreme precipitation) is subject to a high degree of uncertainty. When future projections from the same GCMs were downscaled to local scales, the projected changes in extreme precipitation varied substantially depending on the downscaling algorithm and the observational data used to train the downscaling algorithm. For specific applications, the choice between using MACA or LOCA is therefore important. For example, for emergency planning and infrastructure design crucial for climate change adaptation, it is the extreme events that matter, and the two products differ the most in projecting changes in the intensity and frequency of rare extreme events, with significantly less intense and less frequent precipitation extremes in LOCA than in MACA.

The substantial differences between MACA and LOCA in projecting changes of extreme precipitation highlight the challenges local and regional climate assessment efforts face to provide reliable local climate projections to support adaptation. In addition to the major sources of uncertainties in global climate projections (emission scenario, model dependence, and internal variability), downscaling techniques also imbue uncertainties in local and regional projections like MACA and LOCA. Subtle processes in statistical downscaling such as tail/trace adjustments or the stage at which bias correction is applied can introduce a large range of uncertainties to the skill of a downscaling product in capturing the frequency and intensity of precipitation extremes (Ahmed et al. 2013; Wootten et al. 2017; Wootten 2018). Further development and improvement of the downscaling techniques are critically needed to provide reliable local climate projections to meet the increasing need for locally relevant climate information to support adaptation (Bierbaum et al. 2013; Kirchhoff et al. 2019). In the long term, as the capacity of high performing computers increases, dynamical downscaling using fine-resolution regional climate models (e.g., Prein et al. 2017) or variable-resolution regionally refined global models (e.g., Energy Exascale Earth System Model; Golaz et al. 2019) are becoming more feasible and may be more regularly used in the future (e.g., Leung et al. 2013). However, all models suffer from systematic biases, which necessitates bias correction for both regional and global climate models (Ahmed et al. 2013; Wang et al. 2017b). As such, high-quality high-resolution precipitation measurement and improvement of bias correction techniques are also critical for producing reliable local-scale climate data in support of future climate adaptation efforts.

Acknowledgments. Wang, Kirchhoff, Seth, and Ding were supported by a grant from the Connecticut Institute for Resilience and Climate Adaptation, and a municipal planning grant from the United States Department of Housing and Urban Development via the Connecticut Department of Public Health. Fomenko was supported by a Department of Education Graduate Assistantship in Areas of National Needs (GAANN) Grant (P200A150311). Constructive comments from three anonymous reviewers have contributed significantly to improving the quality of the paper.

REFERENCES

Abatzoglou, J. T., 2013: Development of gridded surface meteorological data for ecological applications and modelling. *Int. J. Climatol.*, **33**, 121–131, https://doi.org/10.1002/joc.3413.

——, and T. J. Brown, 2012: A comparison of statistical downscaling methods suited for wildfire applications. *Int. J. Climatol.*, **32**, 772–780, https://doi.org/10.1002/joc.2312.

Ahmadalipour, A., and H. Moradkhani, 2017: Analyzing the uncertainty of ensemble-based gridded observations in land surface simulations and drought assessment. *J. Hydrol.*, **555**, 557–568, https://doi.org/10.1016/j.jhydrol.2017.10.059.

Ahmed, K. F., G. Wang, J. Silander, M. A. Wilson, J. M. Allen, R. Horton, and R. Anyah, 2013: Statistical downscaling and bias correction of climate model outputs for climate change impact assessment in the U.S. Northeast. *Global Planet. Change*, **100**, 320–332, https://doi.org/10.1016/j.gloplacha.2012.11.003.

Alder, J. R., and S. W. Hostetler, 2019: The dependence of hydroclimate projections in snow-dominated regions of the western United States on the choice of statistically downscaled climate data. *Water Resour. Res.*, **55**, 2279–2300, https://doi.org/10.1029/2018WR023458.

Badger, A. M., B. Livneh, M. P. Hoerling, and J. K. Eischeid, 2018: Understanding the 2011 Upper Missouri River Basin floods in the context of a changing climate. *J. Hydrol.*, **19**, 110–123, https://doi.org/10.1016/j.ejrh.2018.08.004.

Bierbaum, R., and Coauthors, 2013: A comprehensive review of climate adaptation in the United States: More than before, but less than needed. *Mitigation Adapt. Strategies Global Change*, **18**, 361–406, https://doi.org/10.1007/s11027-012-9423-1.

Brown, P. J., R. S. Bradley, and F. T. Keimig, 2010: Changes in extreme climate indices for the northeastern United States, 1870–2005. *J. Climate*, **23**, 6555–6572, https://doi.org/10.1175/2010JCLI3363.1.

Bureau of Reclamation, 2013: Downscaled CMIP3 and CMIP5 climate and hydrology projections: Release of downscaled CMIP5 climate projections, comparison with preceding information, and summary of user needs'. Technical Services Center, Bureau of Reclamation, U.S. Department of the Interior, 47pp.

Bürger, G., T. Q. Murdock, A. T. Werner, S. R. Sobie, and A. J. Cannon, 2012: Downscaling extremes—An intercomparison of multiple statistical methods for present climate. *J. Climate*, **25**, 4366–4388, https://doi.org/10.1175/JCLI-D-11-00408.1.

Bürger, S. R., S. R. Sobie, A. J. Cannon, A. T. Werner, and T. Q. Murdock, 2013: Downscaling extremes: An intercomparison of multiple methods for future climate. *J. Climate*, **26**, 3429–3449, https://doi.org/10.1175/JCLI-D-12-00249.1.

Cash, D., W. C. Clark, F. Alcock, N. M. Dickson, N. Eckley, and J. Jäger, 2003: Salience, credibility, legitimacy and boundaries: Linking research, assessment and decision making. John F. Kennedy School of Government at Harvard University,

Faculty Working Papers Series RWP02-046, 26 pp., http://nrs.harvard.edu/urn-3:HUL.InstRespos:32067415.

Daly, C., R. P. Neilson, and D. L. Phillips, 1994: A statistical-topographic model for mapping climatological precipitation over mountainous terrain. *J. Appl. Meteor.*, **33**, 140–158, https://doi.org/10.1175/1520-0450(1994)033<0140:ASTMFM>2.0.CO;2.

Deser, C., R. Knutti, S. Solomon, and A. S. Philips, 2012: Communication of the role of natural variability in future North American climate. *Nat. Climate Change*, **2**, 775–779, https://doi.org/10.1038/nclimate1562.

d'Orgeville, M., W. R. Peltier, A. R. Erler, and J. Gula, 2014: Climate change impacts on Great Lakes Basin precipitation extremes. *J. Geophys. Res. Atmos.*, **119**, 10 799–10 812, https://doi.org/10.1002/2014JD021855.

Easterling, D. R., and Coauthors, 2017: Precipitation change in the United States. *Climate Science Special Report: Fourth National Climate Assessment*, D. J. Wuebbles et al., Eds., Vol. I, U. S. Global Change Research Program, 207–230.

Fischer, E. M., and R. Knutti, 2016: Observed heavy precipitation increase confirms theory and early models. *Nat. Climate Change*, **6**, 986–991, https://doi.org/10.1038/nclimate3110.

Fowler, H. J., S. Blenkinsop, and C. Tebaldi, 2007: Linking climate change modelling to impacts studies: Recent advances in downscaling techniques for hydrological modelling. *Int. J. Climatol.*, **27**, 1547–1578, https://doi.org/10.1002/joc.1556.

Frich, P., L. V. Alexander, P. Della-Marta, B. Gleason, M. Haylock, A. M. G. Klein Tank, and T. Peterson, 2002: Observed coherent changes in climatic extremes during the second half of the twentieth century. *Climate Res.*, **19**, 193–212, https://doi.org/10.3354/cr019193.

Giorgi, F., 2019: Thirty years of regional climate modeling: Where are we and where are we going next? *J. Geophys. Res. Atmos.*, **124**, 5696–5723, https://doi.org/10.1029/2018JD030094.

——, C. Jones, and G. R. Asrar, 2009: Addressing climate information needs at the regional level: The CORDEX framework. *WMO Bull.*, **58**, 175–183.

Golaz, J.-C., and Coauthors, 2019: The DOE E3SM coupled model version 1: Overview and evaluation at standard resolution. *J. Adv. Model. Earth Syst.*, **11**, 2089–2129, https://doi.org/10.1029/2018MS001603.

Griffiths, M. L., and R. S. Bradley, 2007: Variations of twentieth-century temperature and precipitation extreme indicators in the northeast United States. *J. Climate*, **20**, 5401–5417, https://doi.org/10.1175/2007JCLI1594.1.

Groisman, P. Ya., R. W. Knight, T. R. Karl, D. R. Easterling, B. Sun, and J. M. Lawrimore, 2004: Contemporary changes of the hydrological cycle over the contiguous United States: Trends derived from in situ observations. *J. Hydrometeor.*, **5**, 64–85, https://doi.org/10.1175/1525-7541(2004)005<0064:CCOTHC>2.0.CO;2.

——, R. Knight, D. R. Easterling, T. R. Karl, G. Hegerl, and V. Razuvaev, 2005: Trends in intense precipitation in the climate record. *J. Climate*, **18**, 1326–1350, https://doi.org/10.1175/JCLI3339.1.

Gutmann, E., T. Pruitt, M. P. Clark, L. Brekke, J. R. Arnold, D. A. Raff, and R. M. Rasmussen, 2014: An intercomparison of statistical downscaling methods used for water resource assessments in the United States. *Water Resour. Res.*, **50**, 7167–7186, https://doi.org/10.1002/2014WR015559.

Henn, B., A. J. Newman, B. Livneh, C. Daly, and J. D. Lundquist, 2018: An assessment of differences in gridded precipitation datasets in complex terrain. *J. Hydrol.*, **556**, 1205–1219, https://doi.org/10.1016/j.jhydrol.2017.03.008.

Hewitson, B. C., and R. G. Crane, 2006: Consensus between GCM climate change projections with empirical downscaling: Precipitation downscaling over South Africa. *Int. J. Climatol.*, **26**, 1315–1337, https://doi.org/10.1002/joc.1314.

Hodgkins, G. A., and R. W. Dudley, 2011: Historical summer base flow and stormflow trends for New England rivers. *Water Resour. Res.*, **47**, W07528, https://doi.org/10.1029/2010WR009109.

Horton, R., and Coauthors, 2014: Northeast. *Climate Change Impacts in the United States: The Third National Climate Assessment*, J. M. Melillo, T. C. Richmond, and G. W. Yohe, Eds., U.S. Global Change Research Program, 371–395.

Hosking, J. R. M., 1990: L-moments: Analysis and estimation of distributions using linear combinations of order statistics. *J. Roy. Stat. Soc.*, **52B**, 105–124, https://www.jstor.org/stable/2345653.

Janssen, E., D. J. Wuebbles, K. E. Kunkel, S. C. Olsen, and A. Goodmann, 2014: Observational- and model based trends and projections of extreme precipitation over the contiguous United States. *Earth's Future*, **2**, 99–113, https://doi.org/10.1002/2013EF000185.

Joyce, L. A., J. T. Abatzoglou, and D. P. Coulson, 2018: Climate data for RPA 2020 Assessment: MACAv2 (METDATA) historical modeled (1950-2005) and future (2006-2099) projections for the conterminous United States at the 1/24 degree grid scale. Forest Service Research Data Archive, https://doi.org/10.2737/RDS-2018-0014.

Karl, T. R., N. Nicholls, and A. Ghazi, 1999: CLIVAR/GCOS/WMO workshop on indices and indicators for climate extremes: Workshop summary. *Climatic Change*, **42**, 3–7, https://doi.org/10.1023/A:1005491526870.

Karmalkar, A. V., J. M. Thibeault, A. M. Bryan, and A. Seth, 2019: Identifying credible and diverse GCMs for regional climate change studies—case study: Northeastern United States. *Climatic Change*, **154**, 367–386, https://doi.org/10.1007/s10584-019-02411-y.

Keim, B., and B. Rock, 2002: New England region's changing climate. *Preparing for a Changing Climate: New England Regional Assessment Overview*, U.S. Global Change Research Program, University of New Hampshire, 96 pp.

Kharin, V., F. Zwiers, X. Zhang, and M. Wehner, 2013: Changes in temperature and precipitation extremes in the CMIP5 ensemble. *Climatic Change*, **119**, 345–357, https://doi.org/10.1007/s10584-013-0705-8.

Kharin, V. V., G. M. Flato, X. Zhang, N. P. Gillett, F. Zwier, and K. J. Anderson, 2018: Risks from climate extremes change differently from 1.5°C to 2.0°C depending on rarity. *Earth's Future*, **6**, 704–715, https://doi.org/10.1002/2018EF000813.

Kirchhoff, C. J., and Coauthors, 2019: Climate assessment for local action. *Bull. Amer. Meteor. Soc.*, **100**, 2147–2152, https://doi.org/10.1175/BAMS-D-18-0138.1.

Knutti, R., R. Furrer, C. Tebaldi, J. Cermak, and G. A. Meehl, 2010: Challenges in combining projections from multiple climate models. *J. Climate*, **23**, 2739–2758, https://doi.org/10.1175/2009JCLI3361.1.

——, D. Masson, and A. Gettelman, 2013: Climate model genealogy: Generation CMIP5 and how we got there. *Geophys. Res. Lett.*, **40**, 1194–1199, https://doi.org/10.1002/grl.50256.

Kotamarthi, R., L. Mearns, K. Hayhoe, C. Castro, and D. Wuebbles, 2016: *Use of Climate Information for Decision-Making and Impact Research*. Strategic Environment Research and

Development Program Rep., U.S. Department of Defense, 55 pp.

Kunkel, K. E., and Coauthors, 2013: Regional climate trends and scenarios for the U.S. National Climate Assessment: Part 1—Climate of the Northeast U.S., NOAA Tech. Rep. NESDIS 142-1, 80 pp., https://www.nesdis.noaa.gov/sites/default/files/asset/document/NOAA_NESDIS_Tech_Report_142-1-Climate_of_the_Northeast_US.pdf.

Leung, L. R., T. Ringler, W. D. Collins, M. Taylor, and M. Ashfaq, 2013: A hierarchical evaluation of regional climate simulations. *Eos, Trans. Amer. Geophys. Union*, **94**, 297–298, https://doi.org/10.1002/2013EO340001.

Livneh, B. T. J., D. W. Bohn, F. Pierce, B. Munoz-Arriola, R. Nijssen, R. Vose, and L. Brekke, 2015: A spatially comprehensive, hydrometeorological data set for Mexico, the US, and southern Canada 1950–2013. *Sci. Data*, **2**, 150042, https://doi.org/10.1038/sdata.2015.42.

Mach, K. J., and C. B. Field, 2017: Toward the next generation of assessment. *Annu. Rev. Environ. Resour.*, **42**, 569–597, https://doi.org/10.1146/annurev-environ-102016-061007.

Mabey, N., J. Gulledge, B. Finel, and K. Silverthorne, 2011: Degrees of Risk: Defining a Risk Management Framework for Climate Security. E3G Rep., 177 pp., https://www.c2es.org/document/degrees-of-risk-defining-a-risk-management-framework-for-climate-security/.

Maraun, D., and Coauthors, 2010: Precipitation downscaling under climate change: Recent development to bridge the gap between dynamical models and the end user. *Rev. Geophys.*, **48**, RG3003, https://doi.org/10.1029/2009RG000314.

Masson, D., and R. Knutti, 2011: Spatial-scale dependence of climate model performance in the CMIP3 ensemble. *J. Climate*, **24**, 2680–2692, https://doi.org/10.1175/2011JCLI3513.1.

Maurer, E. P., H. G. Hidalgo, and T. Das, 2010: The utility of daily large-scale climate data in the assessment of climate change impacts on daily streamflow in California. *Hydrol. Earth Syst. Sci.*, **14**, 1125–1138, https://doi.org/10.5194/hess-14-1125-2010.

McSweeney, C. F., R. G. Jones, R. W. Lee, and D. P. Rowell, 2015: Selecting CMIP5 GCMs for downscaling over multiple regions. *Climate Dyn.*, **44**, 3237–3260, https://doi.org/10.1007/s00382-014-2418-8.

Mearns, L. O., and Coauthors, 2012: The North American Regional Climate Change Assessment Program: Overview of phase I results. *Bull. Amer. Meteor. Soc.*, **93**, 1337–1362, https://doi.org/10.1175/BAMS-D-11-00223.1.

Miao, C. Q., and Coauthors, 2014: Assessment of CMIP5 climate models and projected temperature changes over northern Eurasia. *Environ. Res. Lett.*, **9**, 055007, https://doi.org/10.1088/1748-9326/9/5/055007.

Mizukami, N., and Coauthors, 2016: Implications of the methodological choices for hydrologic portrayals of climate change over the contiguous United States: Statistically downscaled forcing data and hydrologic models. *J. Hydrometeor.*, **17**, 73–98, https://doi.org/10.1175/JHM-D-14-0187.1.

Ning, L., M. E. Mann, R. Crane, T. Wagener, R. G. Najjar Jr., and R. Singh, 2012: Probabilistic projections of anthropogenic climate change impacts on precipitation for the mid-Atlantic region of the United States. *J. Climate*, **25**, 5273–5291, https://doi.org/10.1175/JCLI-D-11-00565.1.

——, E. Riddle, and R. S. Bradley, 2015: Projected changes in climate extremes over the northeastern United States. *J. Climate*, **28**, 3289–3310, https://doi.org/10.1175/JCLI-D-14-00150.1.

Northeast Climate Adaptation Science Center, 2018: Massachusetts Climate Change Projections. Resilient MA Climate Change Clearinghouse for the Commonwealth (resilient MA), accessed May 2018, http://www.resilientma.org/resources/resource:2152.

Pierce, D. W., T. P. Barnett, B. D. Santer, and P. J. Gleckler, 2009: Selecting global climate models for regional climate change studies. *Proc. Natl. Acad. Sci.*, **106**, 8441–8446, https://doi.org/10.1073/pnas.0900094106.

——, and Coauthors, 2013: The key role of heavy precipitation events in climate model disagreements of future annual precipitation changes in California. *J. Climate*, **26**, 5879–5896, https://doi.org/10.1175/JCLI-D-12-00766.1.

——, D. R. Cayan, and B. L. Thrasher, 2014: Statistical downscaling using localized constructed analogs (LOCA). *J. Hydrometeor.*, **15**, 2558–2585, https://doi.org/10.1175/JHM-D-14-0082.1.

——, ——, E. P. Maurer, J. T. Abatzoglou, and K. C. Hegewisch, 2015: Improved bias correction techniques for hydrological simulations of climate change. *J. Hydrometeor.*, **16**, 2421–2442, https://doi.org/10.1175/JHM-D-14-0236.1.

Polade, S. D., D. W. Pierce, D. R. Cayan, A. Gershunov, and M. D. Dettinger, 2014: The key role of dry days in changing regional climate and precipitation regimes. *Sci. Rep.*, **4**, 4364, https://doi.org/10.1038/srep04364.

Prein, A. F., R. M. Rasmussen, K. Ikeda, C. Liu, M. P. Clark, and G. J. Holland, 2017: The future intensification of hourly precipitation extremes. *Nat. Climate Change*, **7**, 48–52, https://doi.org/10.1038/nclimate3168.

Ruti, P. M., and Coauthors, 2016: The MED-CORDEX initiative for Mediterranean climate studies. *Bull. Amer. Meteor. Soc.*, **97**, 1187–1208, https://doi.org/10.1175/BAMS-D-14-00176.1.

Sanford, T., P. C. Frumhoff, A. Luers, and J. Gulledge, 2014: The climate policy narrative for a dangerously warming world. *Nat. Climate Change*, **4**, 164–166, https://doi.org/10.1038/nclimate2148.

Seth, A., and Coauthors, 2019: Connecticut Physical Climate Science Assessment Report (PCSAR). Connecticut Institute for Resilience and Climate Adaptation (CIRCA), 74 pp., https://circa.uconn.edu/wp-content/uploads/sites/1618/2019/08/CTPCSAR-Aug2019.pdf.

Sheffield, J., and Coauthors, 2013: North American climate in CMIP5 experiments. Part I: Evaluation of historical simulations of continental and regional climatology. *J. Climate*, **26**, 9209–9245, https://doi.org/10.1175/JCLI-D-12-00592.1.

Stoner, A., K. Hayhoe, and X. Yang, 2012: An asynchronous regional regression model for statistical downscaling of daily climate variables. *Int. J. Climatol.*, **33**, 2473–2494, https://doi.org/10.1002/joc.3603.

Tebaldi, C., J. M. Arblaster, and R. Knutti, 2011: Mapping model agreement on future climate projections. *Geophys. Res. Lett.*, **38**, L23701, https://doi.org/10.1029/2011GL049863.

Thibeault, J., and A. Seth, 2014: Changing climate extremes in the Northeast United States: Observations and projections from CMIP5. *Climatic Change*, **127**, 273–287, https://doi.org/10.1007/s10584-014-1257-2.

Trenberth, K., 1999: Conceptual framework for changes of extremes of the hydrologic cycle with climate change. *Climatic Change*, **42**, 327–339, https://doi.org/10.1023/A:1005488920935.

Walsh, J., and Coauthors, 2014: Our changing climate. *Climate Change Impacts in the United States: The Third National Climate Assessment*, J. M. Melillo, T. C. Richmond, and G. W. Yohe, Eds., U.S. Global Change Research Program, 19–67.

Wang, G., D. Wang, K. E. Trenberth, M. Yu, A. Erfanian, M. Bosilovich, and D. Parr, 2017a: The peak structure and future changes of the relationships between extreme precipitation

and temperature. *Nat. Climate Change*, **7**, 268–274, https://doi.org/10.1038/nclimate3239.

——, K. F. Ahmed, L. You, M. Yu, J. S. Pal, and Z. M. Ji, 2017b: Projecting regional climate and cropland changes using a linked biogeophysical-socioeconomic modeling framework. Part 1: Model description and an equilibrium application. *J. Adv. Model. Earth Syst.*, **9**, 354–376, https://doi.org/10.1002/2016MS000712.

Wilby, R. L., and S. Dessai, 2010: Robust adaptation to climate change. *Weather*, **65**, 180–185, https://doi.org/10.1002/wea.543.

Wood, A. W., L. R. Leung, V. Sridhar, and D. P. Lettenmaier, 2004: Hydrologic implications of dynamical and statistical approaches to downscaling climate model outputs. *Climatic Change*, **62**, 189–216, https://doi.org/10.1023/B:CLIM.0000013685.99609.9e.

Wootten, A., 2018: The subtle processes in statistical downscaling and the potential uncertainty. *U.S. CLIVAR Variations*, Vol. 16, No. 3, International CLIVAR Project Office, Southampton, United Kingdom, 8–13, https://usclivar.org/newsletter/newsletters.

——, A. Terando, B. J. Reich, R. P. Boyles, and F. Semazzi, 2017: Characterizing source of uncertainty from global climate models and downscaling techniques. *J. Appl. Meteor. Climatol.*, **56**, 3245–3262, https://doi.org/10.1175/JAMC-D-17-0087.1.

Zhang, X., L. Alexander, G. C. Hegerl, P. Jones, A. Klein Tank, T. C. Peterson, B. Trewin, and F. W. Zwiers, 2011: Indices for monitoring changes in extremes based on daily temperature and precipitation data. *Wiley Interdiscip. Rev.: Climate Change*, **2**, 851–870, https://doi.org/10.1002/wcc.147.

Zobel, Z., J. Wang, D. J. Wuebbles, and V. R. Kotamarthi, 2018: Analyses for high-resolution projections through the end of the 21st century for precipitation extremes over the United States. *Earth's Future*, **6**, 1471–1490, https://doi.org/10.1029/2018EF000956.